Nanoscale Real-Time Detection of Quantum Vortices at Millikelvin Temperatures

Andrew Guthrie
Lancaster University
Sergey Kafanov (sergey.kafanov@lancaster.ac.uk)
Lancaster University
Mark Noble
Lancaster University
Yuri Pashkin
Lancaster University
George Pickett
Lancaster University
Viktor Tsepelin
Lancaster University https://orcid.org/0000-0001-9978-7832
Alexander Dorofeev
M. V. Lomonosov Moscow State University, Quantum Technology Centre
Vladimir Krupenin
M. V. Lomonosov Moscow State University, Quantum Technology Centre
Denis Presnov
M. V. Lomonosov Moscow State University, D. V. Skobeltsyn Institute of Nuclear Physics
https://orcid.org/0000-0002-9213-0165

Article

Keywords: turbulence, quantum fluids, nanobeams, vorticity density

Posted Date: July 21st, 2020

DOI: https://doi.org/10.21203/rs.3.rs-40690/v1

Version of Record: A version of this preprint was published at Nature Communications on May 11th, 2021. See the published version at https://doi.org/10.1038/s41467-021-22909-3.

Nanoscale Real-Time Detection of Quantum Vortices at Millikelvin Temperatures

A. Guthrie[1], S. Kafanov[1], M. T. Noble[1], Yu. A. Pashkin[1], G. R. Pickett[1] & V. Tsepelin[1]

A. A. Dorofeev[2,3], V. A. Krupenin[2,3] & D. E. Presnov[2,3 4]

[1]*Department of Physics, Lancaster University, Lancaster, LA1 4YB, United Kingdom*

[2]*M. V. Lomonosov Moscow State University, Quantum Technology Centre, Moscow, 119991, Russia*

[3]*M. V. Lomonosov Moscow State University, Faculty of Physics, Moscow, 119991, Russia*

[4]*D. V. Skobeltsyn Institute of Nuclear Physics, M. V. Lomonosov Moscow State University, Moscow, 119991, Russia*

Since we still lack a theory of classical turbulence [1], attention has focused on the conceptually simpler turbulence in quantum fluids. Can such systems of identical singly-quantized vortices provide a physically accessible "toy model" of the classical counterpart? That said, we have hitherto lacked detectors capable of the real-time, non-invasive probing of the wide range of length scales involved in quantum turbulence. However, we demonstrate here the real-time detection of quantum vortices by a nanoscale resonant beam in superfluid ^{4}He at $10\,\mathrm{mK}$. The basic idea is that we can trap a single vortex along the length of a nanobeam and observe the transitions as a vortex is either trapped or released, which we observe through the shift in the resonant frequency of the beam. With a tuning fork source, we can control the ambient vorticity density and follow its influence on the vortex capture and release rates.

But, most importantly, we show that these devices are capable of probing turbulence on the micron scale.

The nanobeams we use for detecting single vortex events in real time have a characteristic dimension less than $1\,\mu\mathrm{m}$ and response times faster than $1\,\mathrm{ms}$. Such devices have recently emerged as highly sensitive probes of hydrodynamic [2,3] and ballistic ^{4}He [4,5]. We present here events demonstrating single-vortex capture, its interaction with the surrounding vortex tangle, and subsequent release via reconnection with a nearby vortex in the surrounding tangle. These measurements advance our capability to probe vortex tangles on much smaller scales than has hitherto been possible.

Figure 1 shows schematically the measurement setup used for the single-vortex detection. Shown in the lower part of the figure, the doubly-clamped, $70\,\mu\mathrm{m}$-long, $\mathrm{Al}-\mathrm{Si_3N_4}$ nanobeam with a $130\,\mathrm{nm}\times 200\,\mathrm{nm}$ cross-section provides the vortex detector. The beam has a vacuum frequency of $2.166\,\mathrm{MHz}$ and is driven at a velocity of only a few millimetres per second. This is orders of magnitude below the expected velocity for the onset of turbulence production [6]. Therefore in all our measurements the beam response is linear and virtually dissipationless. To provide a controlled source of quantum vortices, we use a quartz tuning fork placed $\sim 2\,\mathrm{mm}$ above the beam, driven to a velocity high enough to generate quantum vortices in the ambient superfluid [7,8]. The details of the operating principles and electrical measurement schemes of the fork and nanobeam are described in the Supplementary Information.

Figure 2 shows the time evolution of the response of the nanobeam at each excitation frequency as an example of real-time interactions of the nanobeam with quantum turbulence. The

time trace spans two similar consecutive interaction events. The trace clearly shows that the resonant frequency of the beam shifts significantly (by approximately five widths of the resonance) over a short period of time. We monitor such changes in real-time by the use of a 42-frequency comb produced by a multi-frequency lock-in amplifier[9,10]. The $2\,\mathrm{ms}$ time-analysis interval represents an optimal compromise between fast detection and the frequency resolution of the high-Q resonator.

The pattern of the events in the figure, with the frequency intermittently jumping from a low to a higher value and back again, is maintained over the many hundreds of such interactions we have recorded. Initially the beam frequency is low and stable. At time α (see figure) it gradually increases and stabilises in the region β to γ before abruptly resetting to the initial low-frequency state at time δ. We can identify and associate each change with the successive stages of the nanobeam's interaction with the vortex tangle.

Referring to Fig. 2, the default state of the beam is that with the lowest frequency ($\delta_i\alpha_{i+1}$). This is the only beam response in turbulence-free superfluid, and we identify it with the vortex-free beam. In this state, the beam's resonance frequency is reduced by $50\,\mathrm{kHz}$ from its vacuum value, consistent with the added effective mass contributed by the volume of superfluid displaced.

The damping of the beam in this state, inferred from the resonance width, is identical with that in vacuum. Therefore there is no significant added dissipation mechanisms in the presence of the superfluid, as expected from the low phonon and roton damping at a temperatures of $\sim 10\,\mathrm{mK}$[4].

We believe that the plateau state $\beta_i\gamma_i$, some $\sim 3\,\mathrm{kHz}$ higher than the low state, represents the case where the nanobeam has trapped a singly quantized vortex along its entire length. The state is metastable, but will last for several days in the absence of local turbulence, and survive even if the beam motion is ceased, restarted or even driven quite hard. However, upon restarting the turbulence source, the beam relaxes to the default state with the lower frequency described previously.

The identification of the capture of a singly-quantized vortex by the beam is confirmed by several observations. First, the captive vortex generates two additional restoring forces increasing the beam's resonance frequency; one, the force arising from the vortex interacting with its image in the nearby substrate, and two, the Magnus force.

The interaction of the vortex with a parallel image vortex gives rise to a static force $\boldsymbol{F} = \rho\boldsymbol{v}_s \times \boldsymbol{\kappa}$, with ρ the fluid density, $\boldsymbol{v}_s$ the superflow created by the image at the position of the beam's vortex and $\boldsymbol{\kappa}$ the circulation [11].

The Magnus force arises from the superfluid circulation around the beam acting on the beam's velocity, $\boldsymbol{v}$. This force $\boldsymbol{F}_{\mathrm{M}} = -\rho\boldsymbol{\kappa} \times \boldsymbol{v}$ causes a periodic displacement of the beam orthogonal to its magnetomotively driven direction.

While the extra displacement from either of these forces increases the nanobeam's tension, yielding a higher resonance frequency, we find that the image force dominates since the frequency increase depends only weakly on the beam's velocity. For a fuller description of the forces involved

see the Supplementary Information.

Secondly, the damping of the beam hardly differs from that of the vortex-free or vacuum state, as expected, since the capture of a single vortex should not significantly change the acoustic emission [4], nor should it introduce any new dissipation mechanism. Thirdly, the frequency of the upper plateau is almost always the same ($3\,\mathrm{kHz}$ above the default state), supporting the idea of the capture of a singly-quantized vortex. While double or even higher-order quantization is not energetically unfavourable, it is hard to imagine any creation mechanism. Trapped multiply-quantized vortices would yield discrete higher-frequency plateaus which have not been observed.

We now can attribute the transitions $\alpha_i\beta_i$ and $\gamma_i\delta_i$ between the default and metastable states to the capture and the release of a vortex by the beam. The latter process is always instantaneous on the scale of our detection time and is governed by reconnection of the trapped vortex with a crossing vortex in the surrounding superfluid. The dynamics of the vortex capture by the beam is much more challenging to understand and is clearly a more gradual process. In addition to the "completed" events shown in Fig. 2, we also observe many embryonic cases which never fully develop, rapidly reverting to the default state. Here, the implication is that the vortex does not reach the stable state, either from the failure of some intermediate process, or by premature dislodgement by reconnection with a second vortex.

We should emphasise here that the behaviour of the capture and release processes is completely different. We can show that by looking at the effect of the local vortex density on these two processes.

We begin with the effect on the capture process shown in Fig. 3. The local vortex density is controlled by the velocity of the tuning fork [8]. In panel (**a**) of the figure, we show the tuning fork velocity as a function of the driving force. The clear jump in the slope of the tuning fork response (marking greatly increased dissipation) indicates the onset of turbulence production, see for example references [12,13].

In panel (**a**) we also plot a summary of the single frequency measurements of the detection event rate, τ^{-1}, defined as the inverse mean waiting time τ for an event to occur. The event rate increases with the fork's velocity confirming that the nanobeam probes the surrounding tangle density. We only detect vortices at tangle densities corresponding to fork velocities above $73\,\mathrm{mm\,s^{-1}}$. At this velocity, the rate of detection is very low with the shortest waiting time between the events being $\sim 40\,\mathrm{s}$ and the longest $\sim 1000\,\mathrm{s}$. Panel (**b**) of Fig. 3 presents the probability density function (PDF) of the wait time, $t_{\delta\alpha}$, at five tuning fork velocities showing that the waiting time decreases with increased fork velocity, *i.e.* greater tangle density. The solid lines in the figure correspond to exponential distributions, of the form $\propto \exp(-t_{\delta\alpha}/\tau)$. Since it is known that turbulent tangles emit vortex rings following a similar exponential dependence [14,15], it appears that the capture process may well be governed by the wind of rings emitted by the local tangle. However, whatever the detailed process, it is worth emphasising again that the capture process is governed by the local vortex tangle density.

Once the vortex is captured, its lifetime follows a very different dependence. The release must depend on the proximity of another vortex for annihilation and thus should also carry infor-

mation on the surrounding tangle. Figure 4 shows the probability density function of the measured lifetimes $t_{\alpha\gamma}$ of vortices on the nanobeam at five tuning fork velocities. First, the typical lifetime of a captured vortex state is three orders of magnitude shorter than the wait time between events. Secondly, the data show no discernible dependence on the tuning fork velocity, showing that the release is insensitive to the overall vortex tangle density. This is surprising since we know that the captured state can exist essentially indefinitely if the vorticity is turned off (carefully to avoid dislodging the vortex in the process). Thus, although we understand the "on" and "off" states of the beam, we do not yet fully understand the processes leading to jumps between them.

Since, in the absence of ambient vorticity, the lifetime of the captured vortex is essentially infinite, the release process must be a result of interaction between the captured and external vortices. Although the PDF data of the captive lifetime shown in Fig. 4 is too scattered to indicate its functional form, we can use our range of lifetimes to make some rough estimates of the length scales involved. Optical measurements in superfluid helium [16,17] and simulations of quantum vortex behaviour [18] show that the timescale, t, for vortex-vortex interactions displays a square root relationship with the vortex spacing δ as $\delta = A\sqrt{\kappa\, t_{\alpha\gamma}}$, where κ is the circulation quantum and A a constant of order 1, depending on the geometry of the approaching vortices [17]. This expression and our range of lifetimes of 3 to $100\,\mathrm{ms}$ (as in Fig. 4), suggests an initial vortex separation of 70 to $230\,\mu\mathrm{m}$, in excellent agreement, both with typical vortex tangle densities, and the distances reported by the optical measurements.

In conclusion, we demonstrate that nanobeams can be used as sensitive detectors of single

vortex events, tracking their capture, interaction, and release with millisecond resolution, thereby able to probe the local vortex line density. We foresee that we could readily manufacture multiplexed arrays of such beams with the ability to probe the spatial and temporal evolution of a complex vortex tangle with millisecond resolution and potentially single vortex resolution. Looking further ahead, by capturing a single-vortex in an engineered trapping configuration, we may well be able to study the dynamics of Kelvin waves on the captive vortex, a much anticipated goal in quantum turbulence research [19].

Acknowledgements We thank all members of Lancaster University ULT group as well as A. I. Golov, O. Kolosov, P. V. E. McClintock and W. F. Vinen for helpful discussions. This research was supported by UK EPSRC Grant No. EP/P022197/1 and the EU H2020 European Microkelvin Platform (Grant Agreement 824109). The MSU team was supported by the Russian Science Foundation (Grant 16-12-00072), the research infrastructure of the "Educational and Methodical Center of Lithography and Microscopy", M. V. Lomonosov Moscow State University was used.

Authors' Contributions The nanomechanical samples were fabricated by AAD, VAK and DEP. The idea of the experiment was formulated by AG, SK, MTN, YuAP and VT and performed by AG, SK and MTN. The data analysis was done by AG and MTN. The interpretation of the results performed by AG, SK, MTN, YuAP, GRP and VT. The manuscript is mainly written by AG, MTN, GRP and VT.

Competing Interests The authors declare that they have no competing financial interests.

Correspondence Correspondence and requests for materials should be addressed to Sergey Kafanov (email: sergey.kafanov@lancaster.ac.uk) and Andrew Guthrie (email: a.guthrie1@lancaster.ac.uk)

Online content Statements of data and code availability are available at http://dx.doi.org/10.17635/lancaster/researchdata/xxx.

References

1. The Clay Mathematics Institute, Millennium Problems, Solution to the Navier–Stokes equation. URL https://www.claymath.org/millennium-problems.
2. Bradley, D. I. *et al.* Operating nanobeams in a quantum fluid. *Sci. Rep.* **7**, 4876 (2017).
3. Fong, K. Y., Jin, D., Poot, M., Bruch, A. & Tang, H. X. Phonon coupling between a nanomechanical resonator and a quantum fluid. *Nano Lett.* **19**, 3716 (2019).
4. Guénault, A. M. *et al.* Probing superfluid ^{4}He with high-frequency nanomechanical resonators down to millikelvin temperatures. *Phys. Rev. B* **100**, 020506 (2019).
5. Guénault, A. M. *et al.* Detecting a phonon flux in superfluid ^{4}He by a nanomechanical resonator. *Phys. Rev. B* **101**, 060503 (2020).
6. Hänninen, R. & Schoepe, W. Universal critical velocity for the onset of turbulence of oscillatory superfluid flow. *J. Low Temp. Phys.* **153**, 189 (2008).
7. Bradley, D. I. *et al.* Transition to turbulence for a quartz tuning fork in superfluid ^{4}He. *J. Low Temp. Phys.* **156**, 116 (2009).
8. Jackson, M. J. *et al.* Measurements of vortex line density generated by a quartz tuning fork in superfluid ^{4}He. *J. Low Temp. Phys.* **183**, 208 (2016).
9. Tholén, E. A. *et al.* Note: The intermodulation lockin analyzer. *Rev. Sci. Instrum.* **82**, 026109 (2011).
10. Bradley, D. I. *et al.* Probing liquid ^{4}He with quartz tuning forks using a novel multifrequency lock-in technique. *J. Low Temp. Phys.* **184**, 1080 (2016).

11.Vinen, W. F. The detection of single quanta of circulation in liquid helium ii. *Proc. R. Soc. Lon. Ser.-A* **260**, 218 (1960).

12.Bradley, D. *et al.* Turbulence generated by vibrating wire resonators in superfluid ^{4}He at low temperatures. *J. Low Temp. Phys.* **138**, 493 (2005).

13.Bradley, D. *et al.* Stability of flow and the transition to turbulence around a quartz tuning fork in superfluid ^{4}He at very low temperatures. *Phys. Rev. B* **89**, 214503 (2014).

14.Yano, H. *et al.* Vortex emission from quantum turbulence generated by vibrating wire in superfluid ^{4}He. *J. Low Temp. Phys.* **196**, 184 (2019).

15.Nakagawa, T., Inui, S., Tsubota, M. & Yano, H. Statistical laws and self-similarity of vortex rings emitted from a localized vortex tangle in superfluid ^{4}He. *Phys. Rev. B* **101**, 184515 (2020).

16.Bewley, G., Paoletti, M., Sreenivasan, K. & Lathrop, D. Characterization of reconnecting vortices in superfluid helium. *P. Natl. Acad. Sci. USA* **105**, 13707 (2008).

17.Fonda, E., Sreenivasan, K. R. & Lathrop, D. P. Reconnection scaling in quantum fluids. *P. Natl. Acad. Sci. USA* **116**, 1924 (2019).

18.Galantucci, L., Baggaley, A. W., Parker, N. G. & Barenghi, C. F. Crossover from interaction to driven regimes in quantum vortex reconnections. *P. Natl. Acad. Sci. USA* **116**, 12204 (2019).

19.Eltsov, V. B. & L'vov, V. S. Amplitude of waves in the kelvin-wave cascade. *Pis'ma v ZhETF* **111**, 462 (2020).

20.Holt, S. & Skyba, P. Electrometric direct current I/V converter with wide bandwidth. *Rev. Sci. Instrum.* **83**, 064703 (2012).

Figure Legends

Figure 1 (Colour online) Schematic of the experimental setup. A tuning fork generates quantum turbulence, whilst a 70 µm-long nanomechanical beam, suspended 1 µm above the substrate, acts as the detector. The beam and fork are driven by vector network analysers or signal generators through several stages of attenuation at various temperatures. The beam and fork signals are amplified at room temperature by a 80 dB amplifier and an I/V converter [20]. For a detailed description see the Supplementary Information.

Figure 2 (Colour online) The magnitude of the nanobeam response at each excitation frequency against time taken from the start of the first event in heat-map format. Before point α_1 the beam is in the default vortex-free state. Between α_1 and β_1 a vortex interacting with the beam gradually raises the beam frequency by 3 kHz, finally becoming captured along the entire length of the beam at β_1. From β_1 to γ_1 the resonance is stable for 20 ms. The captured vortex interacts with a nearby vortex and at point γ_1/δ_1 the system suddenly resets via reconnection of the trapped and attracted vortices and the beam resonance jumps back to the vortex-free state. After 14.35 s a second event at α_2 occurs with similar features. The cartoons along the top of the figure sketch the broad processes involved, although the precise details of the capture and release mechanisms are not completely understood.

Figure 3 (Colour online) **a**. The tuning fork velocity as a function of the applied force on the left axis and the rate of detected events by the beam on the right axis. The blue circles correspond to the tuning fork force-velocity dependence, while the symbols on the right

show the beam detection rate at various fork forces. The dotted blue line corresponds to the onset of turbulence production by the tuning fork. **b**. A probability density function of the wait time between events $t_{\delta\alpha}$ at the same fork velocities. The solid lines correspond to exponential fits, of the form $\propto \exp(-t/\tau)$. Note colour and symbol matching between panels **a** and **b**. For details, see text.

Figure 4 (Colour online) A probability density function (PDF) of captured vortex lifetimes $t_{\alpha\delta}$ at selected fork velocities. The discrete data at long lifetimes are the result of single observed events. The data point colours reflect the same data as in Fig. 3.

Figures

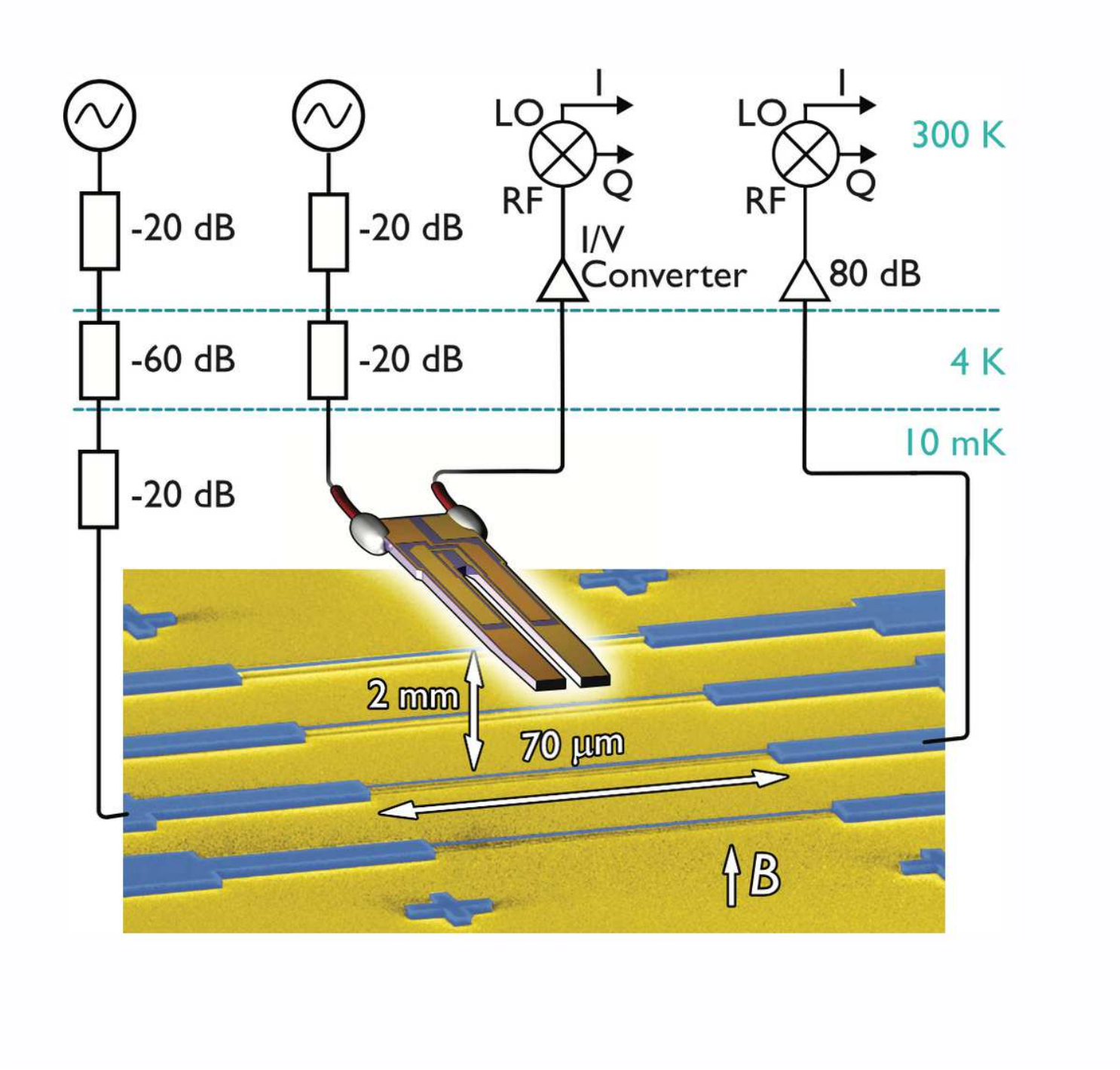

Figure 1

(Colour online) Schematic of the experimental setup. A tuning fork generates quantum turbulence, whilst a 70 µm-long nanomechanical beam, suspended 1 µm above the substrate, acts as the detector. The beam and fork are driven by vector network analysers or signal generators through several stages of attenuation at various temperatures. The beam and fork signals are amplified at room temperature by a 80dB amplifier and an I/V converter 20. For a detailed description see the Supplementary Information.

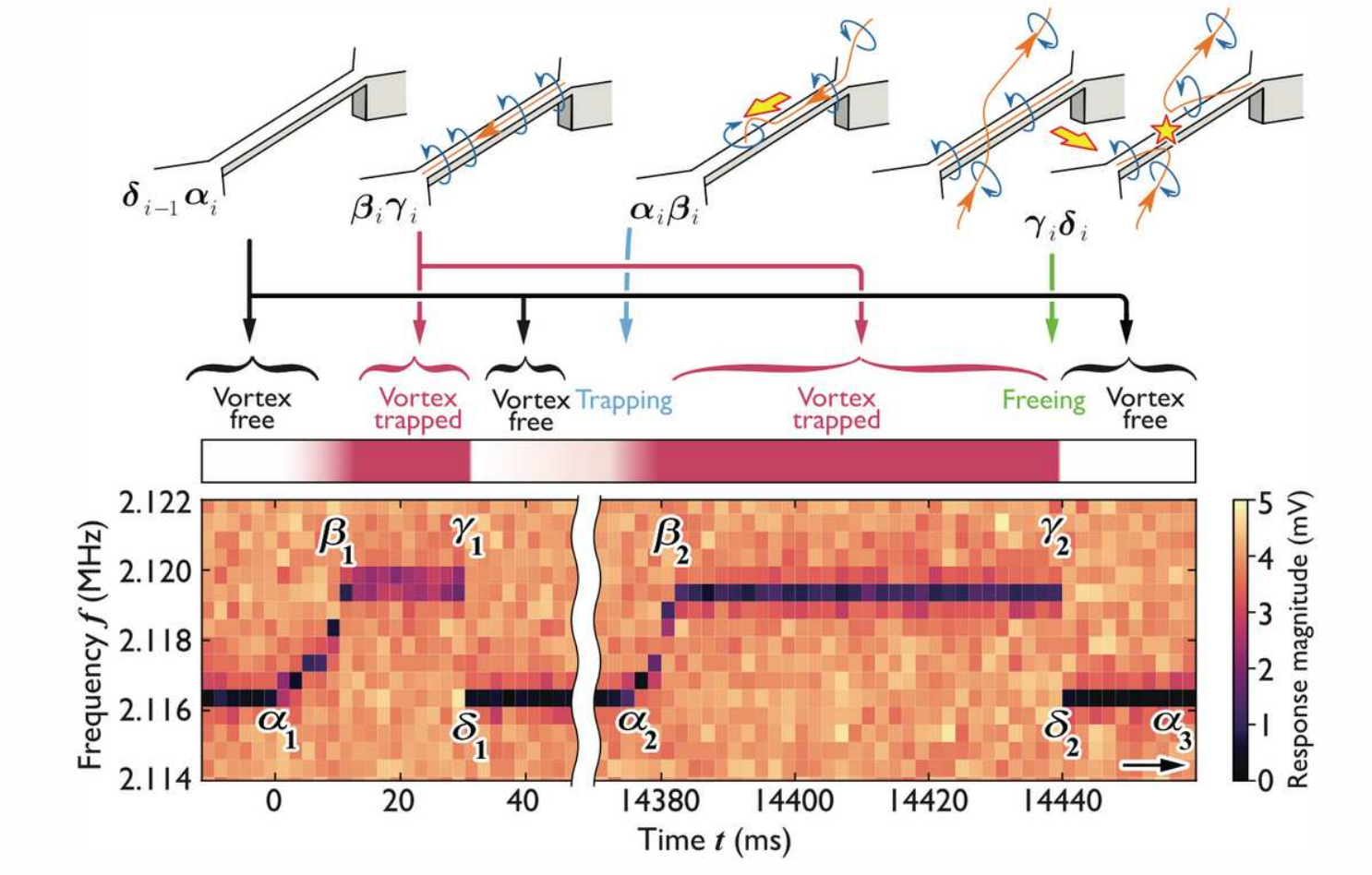

Figure 2

(Colour online) The magnitude of the nanobeam response at each excitation frequency against time taken from the start of the first event in heat-map format. Before point α1 the beam is in the default vortex-free state. Between α1 and β1 a vortex interacting with the beam gradually raises the beam frequency by 3kHz, finally becoming captured along the entire length of the beam at β1. From β1 to γ1 the resonance is stable for 20ms. The captured vortex interacts with a nearby vortex and at point γ1/δ1 the system suddenly resets via reconnection of the trapped and attracted vortices and the beam resonance jumps back to the vortex-free state. After 14.35s a second event at α2 occurs with similar features. The cartoons along the top of the figure sketch the broad processes involved, although the precise details of the capture and release mechanisms are not completely understood.

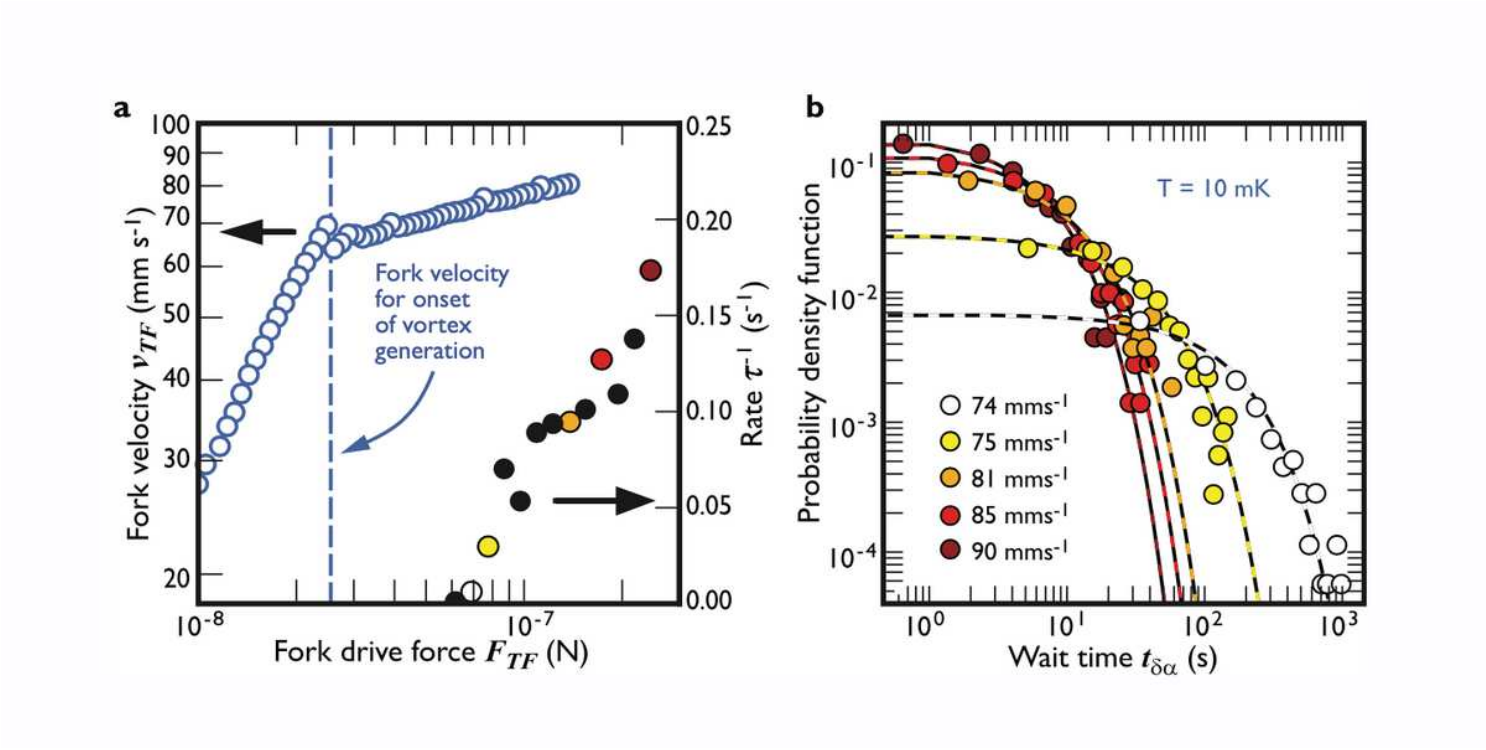

Figure 3

(Colour online) a. The tuning fork velocity as a function of the applied force on the left axis and the rate of detected events by the beam on the right axis. The blue circles correspond to the tuning fork force-velocity dependence, while the symbols on the right show the beam detection rate at various fork forces. The dotted blue line corresponds to the onset of turbulence production by the tuning fork. b. A probability density function of the wait time between events tδα at the same fork velocities. The solid lines correspond to exponential fits, of the form exp(−t/τ). Note colour and symbol matching between panels a and b. For details, see text.

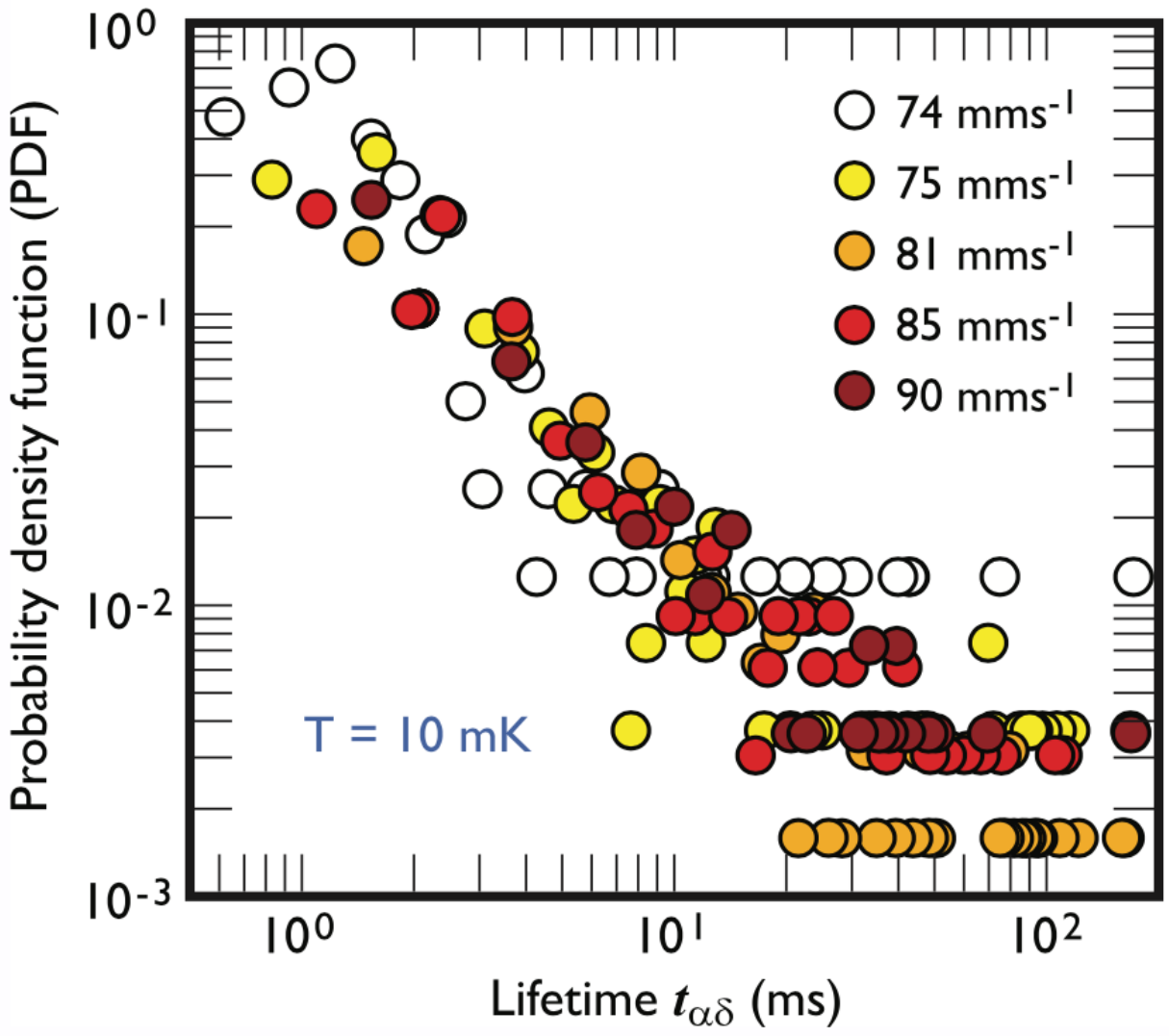

Figure 4

(Colour online) A probability density function (PDF) of captured vortex lifetimes tαδ at selected fork velocities. The discrete data at long lifetimes are the result of single observed events. The data point colours reflect the same data as in Fig. 3.

Supplementary Files

This is a list of supplementary files associated with this preprint. Click to download.

- SupplementaryMaterials.pdf